

CHARACTERIZATION AND CHEMISTRY OF FISSION PRODUCTS RELEASED FROM
LWR FUEL UNDER ACCIDENT CONDITIONS*

K. S. Norwood,** J. L. Collins, M. F. Osborne, R. A. Lorenz, and R. P. Wichner#

CONF-840701--27

ABSTRACT

TI85 016383

Segments from commercial LWR fuel rods have been tested at temperatures between 1400 and 2000°C in a flowing steam-helium atmosphere to simulate severe accident conditions. The primary goals of the tests were to determine the rate of fission product release and to characterize the chemical behavior. This paper is concerned primarily with the identification and chemical behavior of the released fission products with emphasis on antimony, cesium, iodine, and silver. The iodine appeared to behave primarily as cesium iodide and the antimony and silver as elements, while cesium behavior was much more complex.

INTRODUCTION

A series of tests at Oak Ridge National Laboratory (ORNL) is being conducted to measure fission product release rates from commercial, irradiated LWR fuel under idealized accident conditions; to determine the physical and chemical forms of released materials; to compare the results with NUREG-0772 (1) (a 1981 NRC technical review) and with the SASCHA tests (simulated core melt tests being conducted in Germany); and to determine the physical and chemical changes in the fuel specimen. The current program is an extension of a previous fission product release program (2-4). In the present program (5-7), LWR fuel specimens have been tested in the temperature range of 1670 to 2270 K in a flowing steam-helium (or steam-argon)

*Research sponsored by the Office of Nuclear Regulatory Research, U.S. Nuclear Regulatory Commission under Interagency Agreement 40-551-75 with the U.S. Department of Energy under contract DE-AC05-84OR21400 with the Martin Marietta Energy Systems, Inc.

**Guest scientist from UKAEA.

#Members of Chemical Technology Division, Oak Ridge National Laboratory, Oak Ridge, TN 37831.

By acceptance of this article, the publisher or recipient acknowledges the U.S. Government's right to retain a nonexclusive, royalty-free license in and to any copyright covering the article.

MASTER

atmosphere. In the near future, specimens will be heated to ~2670 K. This paper is devoted primarily to the identification and chemical behavior of the released fission products with emphasis on antimony, cesium, iodine, and silver. A more detailed discussion of this work is reported separately (8).

APPARATUS AND ANALYTICAL METHODS

In these tests a collection system was used to characterize the released materials. It was composed of a thermal gradient tube (TGT) lined with platinum foil, followed by a filter pack containing a glass wool prefilter, two HEPA filter papers, and triethylenediamine impregnated charcoal. The TGT was controlled to give a temperature drop from ~1170 K at the inlet to ~420 K at the outlet; fission product condensation behavior depends on volatility, concentration, reactivity, and transit time down the tube (in these tests, 40 to 100 ms). The filters in the filter pack collected particulate material, and the impregnated charcoal trapped more volatile forms, such as elemental iodine and organic iodides. Beyond the filter pack, an ice-bath cooled condenser collected the steam, and charcoal traps at 195 or 77 K sorbed the fission product gases krypton and xenon.

The primary analytical methods for identifying and quantifying released fission products have been gamma spectrometric analysis (GS), neutron activation analysis (NA), spark-source mass spectrometric analysis (SSMS), and scanning electron microscopy with energy dispersive x-ray analysis (EDAX). Fission products that have been identified by the above methods include (GS) ^{137}Cs , ^{134}Cs , ^{125}Sb , ^{85}Kr , ^{106}Ru , $^{110\text{m}}\text{Ag}$, ^{144}Ce , and ^{154}Eu ; (NA) ^{129}I ; (SSMS) and/or (EDAX) Cs, I, Rb, Br, Cd, Te, Ba, and Mo. The SSMS and EDAX analyses were also very useful in identifying nonradiogenic elements from the furnace tube components (ceramics and susceptor) and the fuel cladding that were vaporized and transported along with the fission products to the collectors. The principal contaminants were Mg, S, Cl, Na, Zn, K, W, Zr, Sn, and Pb. Knowledge of the presence or absence of contaminants on collector surfaces is important in the interpretation of chemical behavior.

ANTIMONY RESULTS

Figure 1 illustrates the behavior of antimony in the TGT. These data show that the surface concentration of antimony decreased exponentially with distance from inlet to outlet of the TGT in each of the three tests.

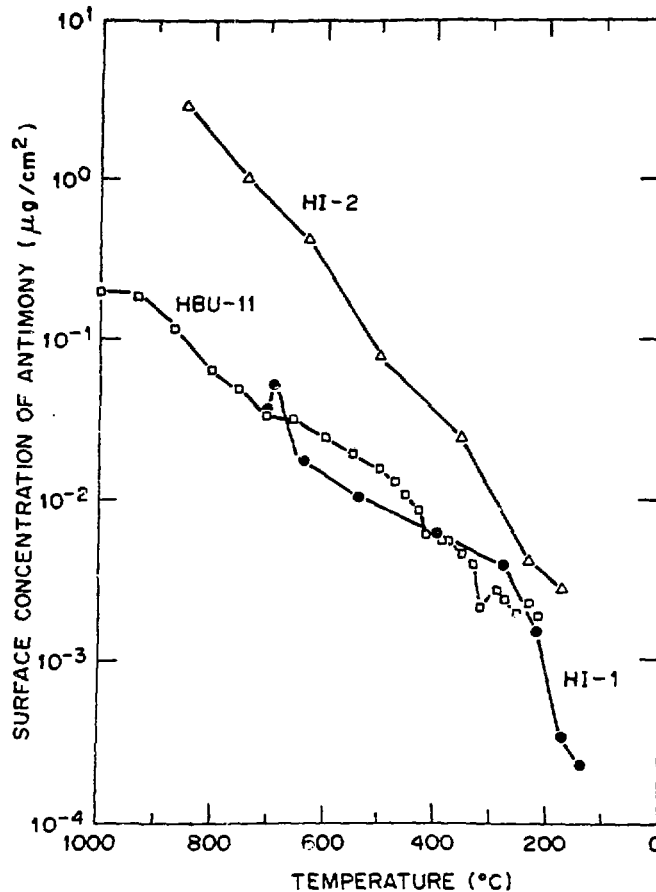


Figure 1. Mass of antimony in thermal gradient tubes after fission product release experiments.

Deposition in the TGT occurred in three stages — movement through the gas to the platinum surface, reaction with the surface, and possibly evaporation back into the gas. The behavior we observed for antimony indicates that diffusion through the gas limited the rate of deposition, while at the surface, antimony reacted rapidly and irreversibly with platinum. This would suggest that antimony was released from fuel and cladding in elemental form. We shall concentrate on the antimony profile from test HI-2 to support this conclusion.

The diffusion coefficient for antimony in a gas mixture can be calculated empirically from the critical temperatures and pressures of all the species involved (9). For antimony, the critical pressure was estimated as 650 bar, and the critical temperature as 2860 K (8). In test HI-2, the calculated diffusion coefficient decreased from 1.7 cm²/s at the inlet to the TGT to 0.3 cm²/s at the outlet. Using

the measured gas flow rate and the temperature profile, the diffusion equation was solved for laminar gas flow (parabolic velocity profile). Figure 2 compares the measured and calculated antimony profiles in test HI-2; the agreement is good, as is the similarity of the calculated and measured amounts of antimony that escaped from the TGT, 0.10 μg and 0.11 μg , respectively.

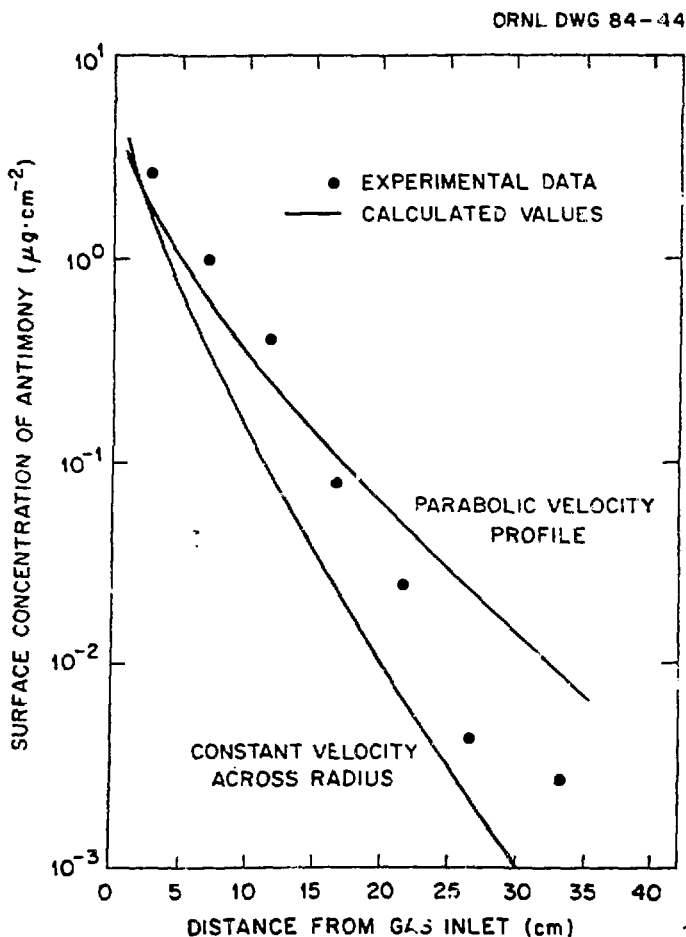


Figure 2. Comparison of measured and calculated antimony profile in thermal gradient tube after test HI-2.

The partial pressure of antimony in the gas passing down the TGT was low, and elemental antimony was not a stable condensed phase until low temperatures were reached. For instance, antimony in test HI-2 entered the TGT at a partial pressure of $\sim 9 \times 10^{-8}$ bar, which is the saturated vapor pressure of elemental antimony at ~ 770 K (9). Since antimony was found on platinum at temperatures up to 1170 K, a process that reduced the chemical activity of antimony in the solid phase apparently

occurred. We believe a combination of reaction between platinum and antimony, and solid-state diffusion of antimony away from the platinum surface is responsible for driving antimony deposition. Antimony is known to form a solid solution and one congruently melting compound with platinum (10), but the diffusion coefficient for antimony in platinum is not known.

Antimony deposited in the high-temperature end of the TGT at partial pressures well below the vapor pressure of the condensed phase at these temperatures (~1136 K) (8). For this to occur, vapor pressure reduction at the platinum surface would have to be affected either by (a) antimony dissolution in platinum and diffusion from the surface or (b) compound formation between antimony and platinum.

The vapor pressure of antimony dissolved in platinum, P_{Sb}^{*Pt} , may be expressed by

$$P_{Sb}^{*Pt} = \gamma_{Sb} N_{Sb} P_0^* \quad (1)$$

where

γ_{Sb} = activity coefficient of Sb dissolved in Pt,

N_{Sb} = mol fraction Sb in Pt at surface,

P_0^* = vapor pressure of Sb.

Test data for run HI-2 (6) indicate that a value of $\gamma_{Sb} N_{Sb} = \sim 10^{-5}$ at the hot end of the TGT would cause a sufficient vapor pressure reduction for deposition to occur. An approximate value for the diffusion coefficient of antimony in platinum required for maintenance of sufficiently low surface concentrations to allow antimony deposition may be estimated using

$$D = \frac{4\pi F^2 t}{\pi(\gamma C)^2} \quad (2)$$

where

D = diffusion coefficient Sb in Pt, cm^2/s ,

C = surface concentration Sb, mol/cm^3 ,

t = test duration, s,

F = flux of Sb to surface, $\text{mol}/\text{cm}^2 \cdot \text{s}$.

The values of F , t , and the requisite surface concentration C (assuming $\gamma = 1$) may be obtained from reported test conditions (5-7). The resulting Sb diffusivities in Pt are shown in Fig. 3 compared with literature values of Sb in Au and Te in Pt. It is seen that without some chemical association of antimony with platinum causing the

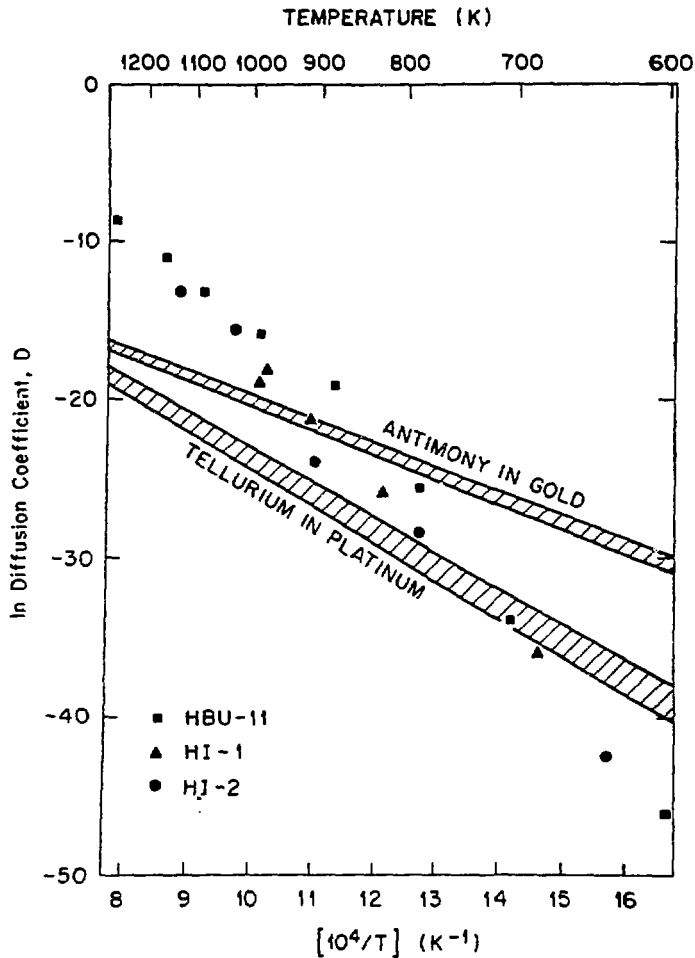


Figure 3. Comparison of the diffusion coefficients for Sb in Au and Pt with the minimum values necessary for tests HI-1, HI-2, and HBU-11.

activity coefficient to be less than unity, the value of D required to maintain sufficiently low surface concentration is greater than reported values for $T > 1000$ K.

However, chemical association is known to occur; platinum reacts with antimony to form PtSb_2 (11), which exists down to 11% mol antimony in platinum. We estimate the enthalpy of formation of PtSb_2 as -63 kJ/mol^{-1} [cf. -77 kJ/mol^{-1} measured for NiSb_2 (ref. 12)] and the entropy change as zero. This implies that $\gamma = 0.36$ at concentrations lower than 0.11 mol fraction. This reduces D by a factor of 10 and brings it closer to measured diffusion coefficients. In conclusion, formation of PtSb_2 in conjunction with solid-state diffusion of antimony is probably sufficient to drive antimony deposition in these experiments.

CESIUM RESULTS

Thermal gradient tube profiles for cesium have generally been complex and made up of several peaks, as illustrated in Fig. 4. The increase in cesium surface concentration below a certain temperature indicates the condensation of a species when its partial pressure exceeds its saturated vapor pressure at that temperature. The surface concentration then decreases downstream as species are removed from the gas.

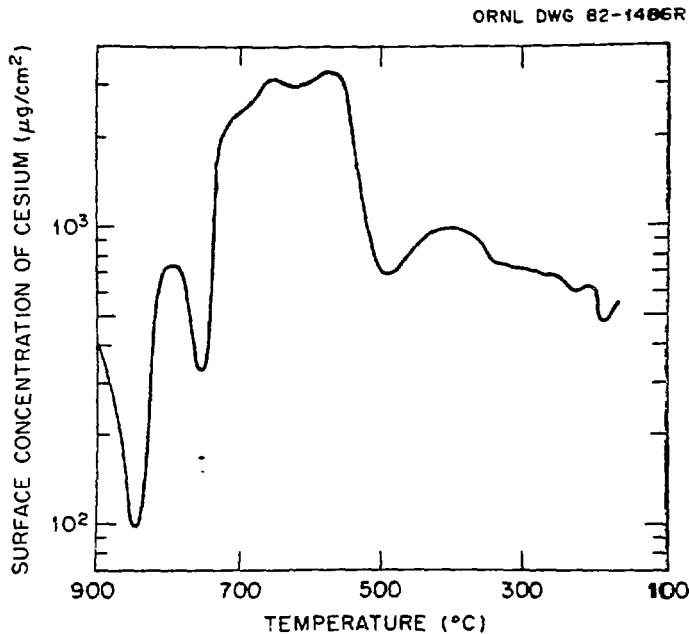


Figure 4. Mass of cesium in thermal gradient tube after test HI-2.

Deposition of vapor onto the platinum surface of the TGT was not the only gas phase removal process (in contrast with the antimony case). Of the cesium that entered the tube, 60 to 70% escaped to the filters as particles. Such a drop in vapor pressure of 30 to 40% cannot produce the drop in surface concentration of 6 to 20 times that was observed. The large drop in vapor pressure must have occurred because cesium compounds condensed as an aerosol in the gas stream as it cooled.

The major cesium compound that deposited in the TGT could not have been CsOH, which is too volatile. For example, in test HI-3 cesium started to deposit at 1040 K but CsOH vapor is calculated to condense at 800 to 850 K, depending on the source of volatility data (13,14). Chemical reactions between CsOH vapor and other previously deposited material may have occurred.

Spark-source mass spectrometry revealed sufficient masses of other elements that could have formed involatile mixed oxides with cesium; these were sulfur (from ceramics in the furnace construction), zirconium (from cladding), molybdenum (fission product), and tungsten (the susceptor in early tests). In addition, the presence of carbon was suspected (from the graphite susceptor used in later tests).

IODINE RESULTS

Iodine TGT profiles have a simple shape, as illustrated in Fig. 5. Table 1 summarizes iodine behavior in the HI test series. Iodine that passed through the filters occurred as a penetrating form, probably I_2 , HI, or CH_3I . In each test, from 0.003 to 0.49% of the total amount of iodine released from the fuel was in a penetrating form. As seen from Table 1, the fraction of iodine entering the TGT that passed through the tube remained relatively constant (57 to 67%) in the HI test series despite a threefold range in gas velocity.

ORNL DWG 83-485

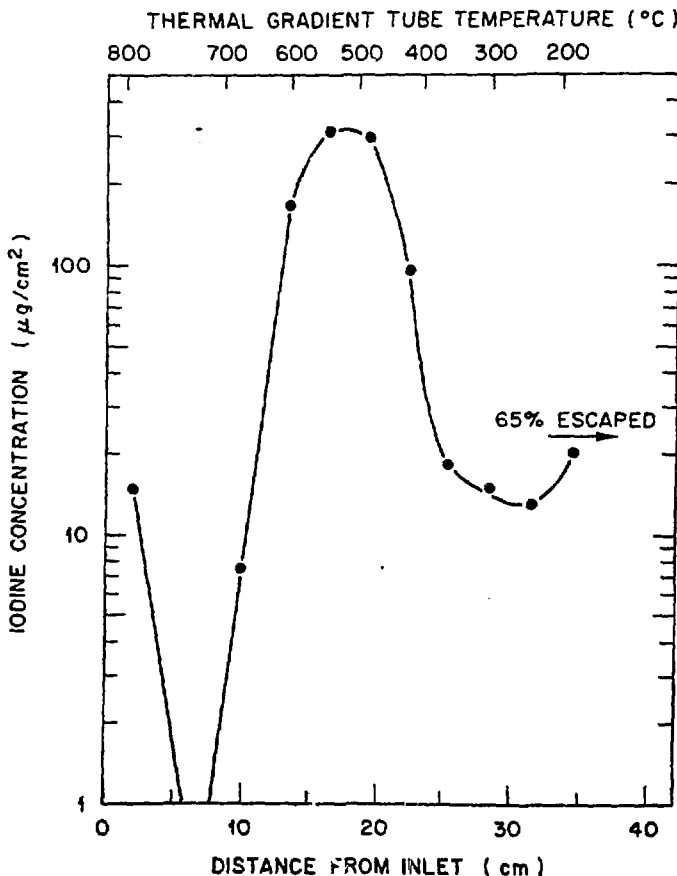


Figure 5. Distribution of iodine in thermal gradient tube in test HI-3.

Table 1

IODINE BEHAVIOR IN THE HI TEST SERIES

<u>Test</u>	<u>Iodine Peak Temperature (K)</u>	<u>Maximum Fuel Temperature (K)</u>	<u>Gas Velocity (mol/min⁻¹)</u>	<u>Iodine Escaping TGT (%)[*]</u>	<u>Iodine in Penetrating Form (%)[*]</u>
HI-1	670	1670	0.06	57	0.49
HI-2	870	1970	0.06	68	0.36
HI-3	840	2270	0.03	65	0.003
HI-4	780	2270	0.03	63	0.03
HI-5	740	2020	0.02	67	0.07

*Percentages of total iodine released from fuel. Total amounts may be twice these because of sorption of I₂ on stainless steel and other surfaces.

Figure 6 compares the location of the peak relative to the predicted location based on CsI vapor pressure and estimated partial pressure of CsI in the TGT. The locations of the upstream edge of the deposition peak for a series of tests (2-7) are plotted in Fig. 6 against the CsI partial pressure estimated from test variables. These locations are compared with two published vapor pressure relationships for CsI (15,16). As seen, the deposit location correlates well with the predicted location for CsI deposition for many of the observations. However, about half the deposit locations occurred at temperatures 50 to 100°C higher than predicted.

SILVER RESULTS

Silver was detected in the TGT in tests HI-2 and HI-5. It appeared to deposit uniformly along the length of the TGT when allowance was made for leaching of silver by basic and acidic leaches. Figure 7 shows the profile for test HI-5.

Because the silver radioactivity was considerably less than the highly active ¹³⁷Cs and ¹³⁴Cs, it was difficult to detect by gamma spectrometry. Consequently, before silver could be measured, the TGT had to be leached with a basic solution (NH₄OH/H₂O₂) and an acidic solution (HNO₃/HF) to remove >90% of the cesium.

No silver was removed by the basic leach, but a small amount was removed by the acid leach at the high temperature end, and considerably more at the low temperature end. The leach behavior is consistent with that of elemental silver.

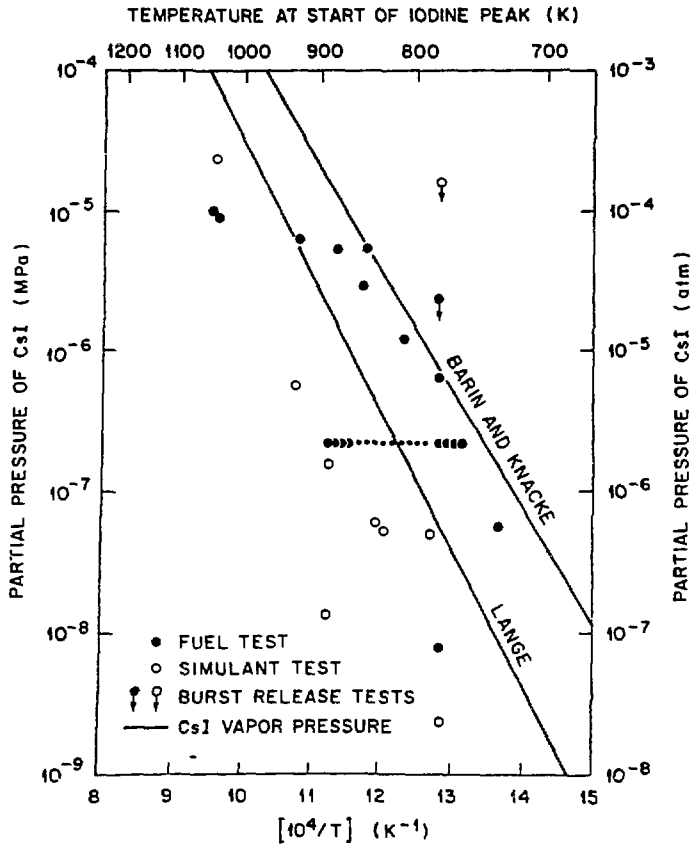


Figure 6. Variation of iodine peak start temperature with CsI partial pressure in ORNL fission product release tests.

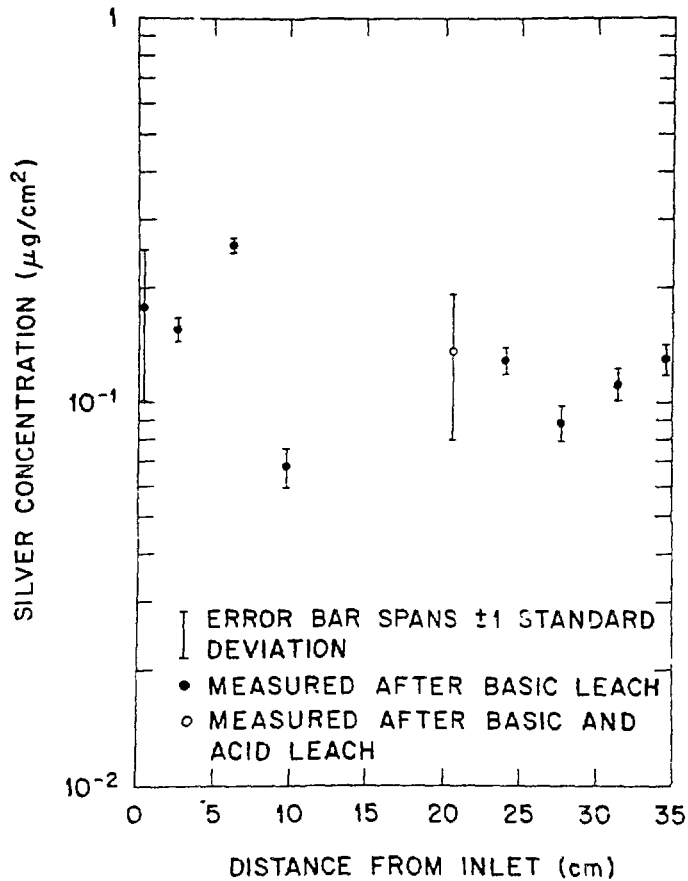


Figure 7. Distribution of silver on thermal gradient tube after test HI-5.

In test HI-5 (and probably in test HI-2), ~80% of the silver that entered the TGT passed through and was collected on the filters. This behavior is typical of an aerosol, which has a low gas diffusivity. Thus, the silver associated with aerosol particles deposited slowly on the platinum surface because the rate was mass transfer limited; the gas phase concentration of silver changed very little and the resulting TGT profiles were flat, with most of the silver collecting downstream on the filters.

These data indicate that silver probably was released from the fuel in the elemental form. If so, the average partial pressure of silver in test HI-5 can be calculated from the mass of silver released and the amount of flowing gas as at least 2.4×10^{-7} bar. This corresponds to a condensation temperature >1120 K (17). It appears that silver began to condense on its own or on aerosol particles just as it entered the TGT.

CONCLUSIONS

When LWR fuel was heated in steam-rich atmospheres, the antimony that was released reacted rapidly and irreversibly with platinum (and gold), as was indicated by the shape of its TGT profiles, and its resistance to basic and acidic leaches. This behavior implies that it was released in the elemental form.

The majority of the cesium was apparently released in an oxidic form, and, in these tests, probably formed mixed oxides with other fission products (Mo, Zr), with structural materials (Zr, W, C), or with impurities in the ceramics (S). Of these elements, only zirconium and molybdenum are likely to be present in a reactor accident. Approximately 10% of the cesium apparently was released as CsI.

About 99.5% of the released iodine was involatile in form; circumstantial evidence points to this being CsI in this series of tests. The apparent deposition velocity of "CsI" onto platinum increases from 0.5 cm/s at 870 ± 50 K to 3.8 cm/s at 670 ± 50 K.

Silver behaved consistently with its release from the fuel in elemental form; apparently, it deposited on surfaces after condensation onto aerosol particles.

REFERENCES

1. Technical Bases for Estimating Fission Product Behavior During LWR Accidents, NUREG-0772, U.S. Nuclear Regulatory Commission, June 1981.
2. R. A. Lorenz, J. L. Collins, A. P. Malinauskas, O. L. Kirkland, and R. L. Towns, Fission Product Release from Highly Irradiated LWR Fuel, NUREG/CR-0722 (ORNL/NUREG/TM-287), February 1980.
3. R. A. Lorenz, J. L. Collins, A. P. Malinauskas, M. F. Osborne, and R. L. Towns, Fission Product Release from Highly Irradiated LWR Fuel Heated to 1300-1600°C in Steam, NUREG/CR-1386 (ORNL/NUREG/TM-346), November 1980.
4. R. A. Lorenz, J. L. Collins, M. F. Osborne, R. L. Towns, and A. P. Malinauskas, Fission Product Release from BWR Fuel Under LOCA Conditions, NUREG/CR-1773 (ORNL/NUREG/TM-388), July 1981.
5. M. F. Osborne, R. A. Lorenz, J. R. Travis, and C. S. Webster, Data Summary Report for Fission Product Release Test HI-1, NUREG/CR-2928 (ORNL/TM-8500), December 1982.
6. M. F. Osborne, R. A. Lorenz, J. R. Travis, C. S. Webster, and K. S. Norwood, Data Summary Report for Fission Product Release Test HI-2, NUREG/CR-3171 (ORNL/TM-8667), February 1984.

7. M. F. Osborne, R. A. Lorenz, K. S. Norwood, J. R. Travis, and C. S. Webster, Data Summary Report for Fission Product Release Test H-3, NUREG/CR-3335 (ORNL/TM-8793), March 1984.
8. K. S. Norwood, An Assessment of Thermal Gradient Tube Results from the HI Series of Fission Product Release Tests, in publication.
9. J. C. Slattery and R. B. Bird, American Institute of Chemical Engineers Journal Vol. 4, 1958, pp. 137-42.
10. I. Barin and O. Knacke, Thermochemical Properties of Inorganic Substances. New York: Springer-Verlag, 1973, p. 659.
11. M. Hansen and K. Anderko, Constitution of Binary Alloys. 2nd ed. New York: McGraw Hill, 1958, p. 1138.
12. R. Hultgren et al., Selected Values of the Thermodynamic Properties of Binary Alloys, American Society for Metals, 1973.
13. M. W. Chase et al., "JANAF Thermochemical Tables 1974 Supplement," Journal of Physical and Chemical Reference Data, Vol. 3, No. 2, 1974, pp. 416-18.
14. Calculation Using Data of R. A. Sallach and R. M. Elrick, Sandia National Laboratory, 1983, personal communication to K. S. Norwood.
15. N. A. Lange, Handbook of Chemistry. 9th ed. New York: McGraw-Hill, 1956, p. 1429.
16. I. Barin and O. Knacke, Thermochemical Properties of Inorganic Substances. New York: Springer-Verlag, 1973, p. 242.
17. R. Hultgren et al., Selected Values of the Thermodynamic Properties of the Elements, p. 21, American Society for Metals, 1973.

DISCLAIMER

This report was prepared as an account of work sponsored by an agency of the United States Government. Neither the United States Government nor any agency thereof, nor any of their employees, makes any warranty, express or implied, or assumes any legal liability or responsibility for the accuracy, completeness, or usefulness of any information, apparatus, product, or process disclosed, or represents that its use would not infringe privately owned rights. Reference herein to any specific commercial product, process, or service by trade name, trademark, manufacturer, or otherwise does not necessarily constitute or imply its endorsement, recommendation, or favoring by the United States Government or any agency thereof. The views and opinions of authors expressed herein do not necessarily state or reflect those of the United States Government or any agency thereof.